

Statistical mechanical approach to secondary processes and structural relaxation in glasses and glass formers

A leading model to describe the onset of Johari-Goldstein processes and their relationship with fully cooperative processes

Andrea Crisanti^{1,2}, Luca Leuzzi^{2,3}, and Matteo Paoluzzi^{3,4}

¹ Dipartimento di Fisica, Università *Sapienza*, Piazzale Aldo Moro, 5 - 00185 - Rome, Italy

² CNR-ISC, Via dei Taurini, 19 - 00185 - Rome, Italy

³ CNR-IPCF, UOS Roma *Kerberos*, Piazzale Aldo Moro, 5 - 00185 - Rome, Italy

⁴ Dipartimento di Fisica, Università Roma Tre, Via della Vasca Navale, 84 - 00184 - Rome, Italy

Received: date / Revised version: date

Abstract. The interrelation of dynamic processes active on separated time-scales in glasses and viscous liquids is investigated using a model displaying two time-scale bifurcations both between fast and secondary relaxation and between secondary and structural relaxation. The study of the dynamics allows for predictions on the system relaxation above the temperature of dynamic arrest in the mean-field approximation, that are compared with the outcomes of the equations of motion directly derived within the Mode Coupling Theory (MCT) for under-cooled viscous liquids. Varying the external thermodynamic parameters a wide range of phenomenology can be represented, from a very clear separation of structural and secondary peak in the susceptibility loss to excess wing structures.

1 Introduction

Secondary processes in supercooled liquids and glasses are related to complicated though local, non- or not fully cooperative, dynamics. They occur on time-scales much slower than cage rattling, but much faster than struc-

tural relaxation. Their existence was first pointed out in the 1960's from the experimental observation of a second peak in dielectric loss spectra at a frequency, $\nu_\beta \sim 1/\tau_\beta$, higher than the frequency $\nu_\alpha \sim 1/\tau_\alpha$ of peak known to represent the structural α relaxation. This so-called β -peak was recorded in glycerol, propyleneglycol, n-propane, dif-

ferent polymeric substances and liquids composed of rigid molecules. Johari and Goldstein eventually conjectured that such processes - now known as Johari-Goldstein (JG) - originate from the same complicated frustrated interactions leading to the glass transition [1,2,3].

Also in cases where spectral density of response losses do not clearly show a second peak, secondary processes can be active and induce some anomaly at high frequency. This feature of the susceptibility loss part is called "excess wing" and was initially observed as an apart phenomenon [4]. Actually, classifications exist in terms of glass formers displaying excess wings and substances showing well defined β -peaks [5,6,7]. Although more recent investigation has provided evidence supporting the idea that the excess wing is not an apart dynamic process, but rather a manifestation of a JG process [8][9] and that tuning proper thermodynamic parameters (temperature, pressure, concentration, ...) the latter can emerge out of the first one (or, viceversa, a secondary peak can reduce to an excess wing). Cummins [10] suggests, e.g., that the relevant parameter may be the rotation - translation coupling constant which becomes stronger as density increases, because of pressure increase or temperature decrease, and is larger for liquid glass former made of elongated, strongly anisotropic molecules. Also theoretical attempts have been carried out in this direction as, for instance, in the framework of Mode Coupling Theory (MCT), by means of which the relaxation of reorientational correlation and rotation-translation coupling in liquids composed of strongly anisotropic molecules appears to be logarithmic in time [11].

A comprehensive picture is, though, not yet established and many questions are open. For instance about the dependence on temperature and pressure (or concentration) of characteristic time scales of JG processes, or the possibility that secondary processes might disclose a certain degree of cooperativeness [12], or the persistence of β processes also below the glass transition temperature T_g [10]. A very interesting question is if there is a straightforward connection, and, in case, which one, between processes evolving at qualitatively different time-scales. Or, rephrased, whether one might devise the long-time behavior of α relaxation from the behaviors of the fast small amplitude cage dynamics (γ processes) and of the (slower) secondary processes.

In glasses, and glass-formers, where α and JG β peaks can be clearly resolved in frequency (e.g., 4-polybutadiene, toluene[13] [14] or sorbitol [15]), one can describe the system in terms of a scenario where two time-scale bifurcations accelerate as temperature is lowered and processes consequently evolve on three "well separated" time sectors.

We, therefore, analyze the dynamic properties of a model for slowly relaxing glassy systems with up to three time-scales. This is a generalization of the p -spin model with quenched disorder, that is known to heuristically reproduce all the basic features of structural glasses [16] [17] [18] [19] and whose dynamics above a certain temperature ("dynamic" or "mode coupling") is equivalent to the dynamics of the schematic mode coupling theory (MCT) with a kernel depending from the correlator as

ϕ^{p-1} [20]. The generalization consists in coupling the dynamical variable spin (playing, e.g., the role of a density fluctuation, or a component of molecular orientation) with other spins in two different ways: as a part of a group of s variables and as a part of a group of p variables. Variables in each group interact among themselves through i.i.d. random multi-body interaction of zero mean and mean square strength of magnitude $\sim J_s$ and J_p , respectively. As one of these two interaction mechanisms (e.g., "p") involves sensitively more dynamical variables than the other (e.g., "s"), this triggers a mixture of strong and weak cooperativeness that can be varied by an external control parameter (e.g, J_p/J_s).

Our aim is to provide a model to interpolate between different resolutions of secondary processes and support the idea that excess wings and secondary peaks are both manifestations of intermediate (slow, yet thermalized) processes between cage rattling and structural relaxation. Relying on the results about correlation functions and spectral densities we can argue on the possible interrelation between processes evolving on different time-scales and their characteristic times, τ_α , τ_β and τ_γ .

2 The leading spin model for secondary processes

The model we will consider is a spherical $s + p$ -spin interaction model:

$$\mathcal{H} = \sum_{i_1 < \dots < i_s} J_{i_1 \dots i_s}^{(s)} \sigma_{i_1} \dots \sigma_{i_s} + \sum_{i_1 < \dots < i_p} J_{i_1 \dots i_p}^{(p)} \sigma_{i_1} \dots \sigma_{i_p} \quad (1)$$

where $J_{i_1 \dots i_t}^{(t)}$ ($t = s, p$) are uncorrelated, zero mean, Gaussian variables of variance $J_t^2 t! / (2N^{t-1})$ and σ_i are N "spherical spins" obeying the constraint $\sum_i \sigma_i^2 = N$. Since every spin interact (very slightly, $J_t \sim 1/N^{(t-1)/2}$) with every other, for this system the mean-field approximation is exact. We will consider the case in which each spin interact with the rest of the system in two different ways: in *small* groups (of s elements) and in *large* group (of p elements). If $p - s$ is large enough standard MCT provides evidence for glass-to-glass transitions beyond the line of validity of time translational invariance [21], that is a fundamental assumption for MCT. The theories developed for quenched disordered systems, allow further to compute the stable solutions corresponding to the glassy phases involved below the dynamic transition and identify the nature of the processes ongoing in each one of the glasses. Eventually, it can be shown that the model thermodynamics displays three distinct glass phases below the line of dynamic arrest, one of which consisting of processes thermalized at three completely separate time-scales [22][23]. Starting from these considerations dynamic equations are obtained, reducing to those of schematic MCT above the mode coupling temperature T_d . We will see that the three time-scale glass will be already signaled in the dynamics following educated paths in the phase diagram.

The glass phase with double bifurcation of time-scales can be yielded in the s - p spherical spin model under a certain condition on the values of s and p , i.e., for a given s , p must be equal or larger than value solution of

$$(p^2 + s^2 + p + s - 3ps)^2 - ps(p-2)(s-2) = 0. \quad (2)$$

as it has been shown in Ref. [22]. Some example of "threshold" couples (s, p) to obtain a double bifurcation are $(3, 8)$, $(4, 11)$ or $(5, 16)$. The larger is $p-s$, the broader the region of phase diagram where double bifurcation can be found.

The external thermodynamic parameters are the temperature and the relative weight of the two interaction terms (big to small) in the Hamiltonian. In unit of J_s : T/J_s and J_p/J_s . These are related to the usual mode-coupling parameters so that the memory kernel of the dynamic equation takes the mode-coupling form

$$\mathcal{K}(\phi) = \mu_s \phi^{s-1} + \mu_p \phi^{p-1} \quad (3)$$

$$\mu_p = p\beta^2 J_p^2/2 \quad (4)$$

$$\mu_s = s\beta^2 J_s^2/2 \quad (5)$$

We stress that as $p-s$ is large, and $s > 2$, the theory we are considering yields qualitatively different results from schematic MCTs with, e.g., $s = 2$ and $p = 3$ [11,24]. Indeed, in schematic MCT with linear and quadratic terms in the kernel a clear separation of time scales is unfeasible and the (possible) thermodynamic glassy phase underneath can only provide an acceleration of time-scales bifurcation, as discussed in Refs. [25,26,21,23].

The strong three-level separation we study can, then, be softened and adapted to less defined structures than the two peaks (e.g., the excess wing), by tuning the external parameters temperature and J_p/J_s , or by choosing s, p model instances with smaller $p-s$.

The model was initially developed to study the nature of polyamorphism and amorphous-to-amorphous transitions. On the static front, the analysis can be carried

out within the framework of Replica Symmetry Breaking (RSB) theory, leading to the identification of low temperature glass phases of different kinds [22]. Below the Kauzmann-like transition line $T(J_p/J_s)$, the model displays both "one-step" RSB solutions, known to reproduce all basic properties of structural glasses [17], and a physically consistent "two-step" solution [22].

Above the Kauzmann transition line, the thermodynamic stable phase is the fluid paramagnetic phase but excited glassy metastable states are present in a large number, growing exponentially with the size N of the system. The configurational entropy of the system is, thus, extensive. Because barriers between minima of the free energy landscape separating local glassy minima grow like some positive power of N in the mean-field approximation, "metastable" states have, actually, an infinite lifetime in the thermodynamic limit and ergodicity breaking occurs as soon as an extensive configurational entropy appears. The highest temperature at which this happens is known as *dynamic* [19], *arrest* [17] or *Mode Coupling* [27] temperature. We shall denote it by T_d . As the temperature is lowered down to T_d the spin-spin time correlation function (analogue of the correlation between density fluctuations) develops a plateau that, eventually, extends to infinite time as $T = T_d$, signaling the breaking of the ergodicity.

In Fig. 1 we display the $(T/J_s, J_p/J_s)$ phase diagram for $s = 3$ and $p = 16$. We will use this specific case throughout the paper, for which strong discrimination of the secondary processes is easily realizable in a relative

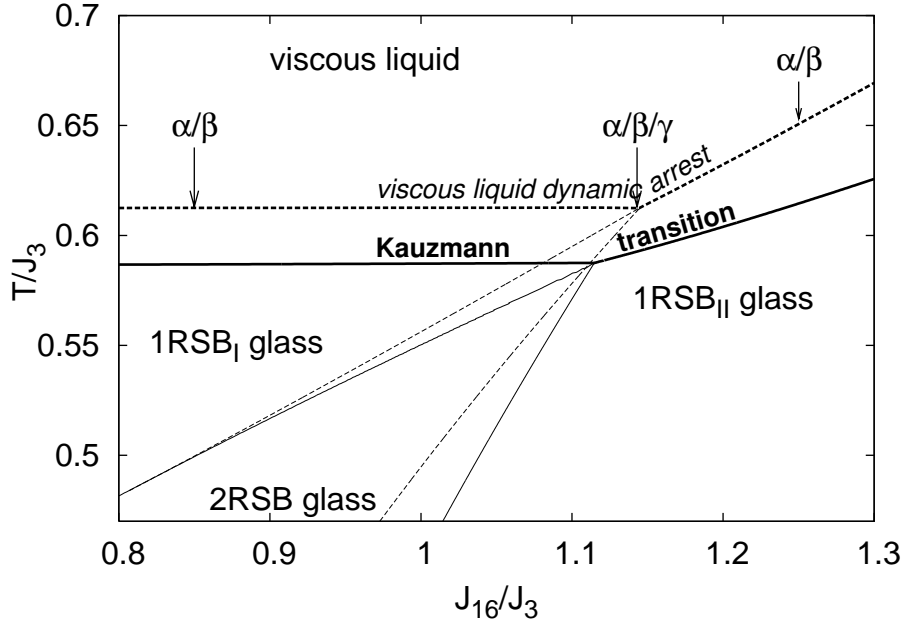


Fig. 1. Phase diagram of the $s = 3$, $p = 16$ spherical spin model. Dynamic transition lines are dashed and thermodynamic transition lines beneath are full. $1RSB_I$ glass stays for a glass with a single time scale bifurcation with relatively low nonergodicity factor for the time correlation function. $1RSB_{II}$ glass stays for a glass with a single time scale bifurcation with higher nonergodicity factor. The $2RSB$ glass displays two bifurcations and two possible correlation values in the arrested state.

wide region of the phase diagram. The dynamic and thermodynamic properties of such an instance below the dynamic transition are discussed in Ref. [28].

2.1 Dynamics

The relaxational dynamic of the system is described by the Langevin equation

$$\Gamma_0^{-1} \frac{\partial \sigma_k(t)}{\partial t} = - \frac{\delta \mathcal{H}[\{\sigma\}]}{\delta \sigma_k(t)} + \eta_k(t) \quad (6)$$

$$\langle \eta_k(t) \eta_n(t') \rangle = 2k_B T \Gamma_0^{-1} \delta_{kn} \delta(t - t')$$

Since the dynamic counterpart of a RSB is known to be a time-scale bifurcation [29,30], Eq. (1) provides a leading model to probe the behavior of characteristic time-scales in presence of secondary processes and the different mechanisms in which they can arise starting from high temperature and cooling down the system.

where η_k is the thermal white noise and Γ_0^{-1} is the microscopic time-scale. Using a Martin-Siggia-Rose path-integral formalism one can reduce the equations of motion to a single variable ($\sigma(t)$) formulation [31,32]. The fundamental observables to study the onset of a slowing down of the dynamics are the time correlation of between the spin variable at time t' and time $t > t'$ and the response func-

tion to a small perturbative field h . For our system they are defined as

$$C(t, t') = \overline{\langle \sigma(t) \sigma(t') \rangle} \quad (7)$$

$$G(t, t') = \frac{\delta \overline{\langle \sigma(t) \rangle}}{\delta \beta h(t')}; \quad t > t' \quad (8)$$

where the overbar denotes the average over quenched disorder, whereas the brackets stay for an average over different trajectories (thermal average). For temperature above T_d the time translational invariance (TTI) holds and the response and correlation functions are related by the Fluctuation - Dissipation Theorem (FDT):

$$G(t - t') = \theta(t - t') \partial_{t'} C(t - t') \quad (9)$$

The dynamic equation of the correlation function then takes the form

$$\Gamma_0^{-1} \frac{\partial C(t)}{\partial t} + \bar{r} C(t) + \int_0^t dt' \Lambda[C(t-t')] \frac{\partial C(t')}{\partial t'} = \bar{r} - 1 \quad (10)$$

with initial condition $C(t=0) = 1$, and

$$\bar{r} = r - \Lambda[C(t=0)] \quad (11)$$

The parameter r is the "bare mass" [33], that for the spherical model is related to the Lagrange multiplier used to impose the spherical constraint [19]. The value of \bar{r} depends on temperature, and $J_{s,p}$; however, in the high temperature phase it is constant and equal to 1, so that the r.h.s. of (10) vanishes.

The function $\Lambda(t) = \Lambda[C(t)]$ is the memory kernel that in the specific case of our model has the functional form:

$$\Lambda(q) = \mu_s q^{s-1} + \mu_p q^{p-1} \quad (12)$$

to be compared with Eq. (3). Indeed, the evolution of the correlation function is described by a dynamical equation

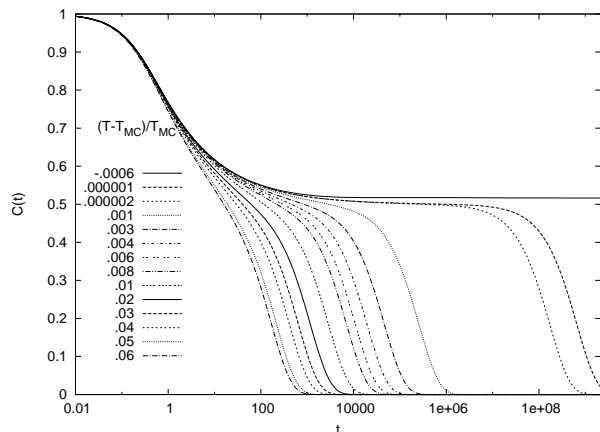


Fig. 2. Correlation function vs. time on log-scale at fixed temperature for the $s = 3$ -spin model, i.e., $J_p = 0$.

equivalent to that of schematic mode-coupling theories, i.e., in which the second order time derivative term in MC equations is replaced by the first order one [20,27].

For $J_s = 0$ one recovers the usual spherical p -spin model [19]. In such model, above T_d the correlation function has the shape plotted in Fig. 2, with one plateau developing for long time.

Cooling down the system and increasing the J_s along certain paths in the phase diagram in order to approach the tricritical point, the time-correlation function develops *two* plateaus at different correlation values, cf. Figs. 3, 4 and 5.

As mentioned above we will denote by γ the fastest relaxation (also referred to as β_{fast} [34]), by β the secondary Johari-Goldstein relaxation (β_{JG}) and by α the structural relaxation. In Fig. 4 we display the behavior of $C(t)$ approaching from high temperature the tricritical point along a $T(J_p)$ line perpendicular to the dynamic transition line with the 1RSB_{II} glass. Changing path, cf. Fig. 5 the qualitative behavior is the same (though quan-

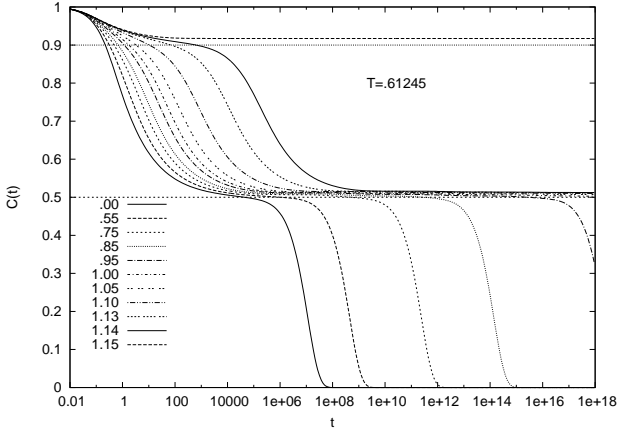


Fig. 3. Correlation function vs. time on log-scale at fixed $T/J_s = 0.61245$ with $s = 3$ and $p = 16$ increasing J_{16} from zero to $J_{16}/J_3 = 1.145$ such that $T_d(J_{16}/J_3) = 0.61245$.

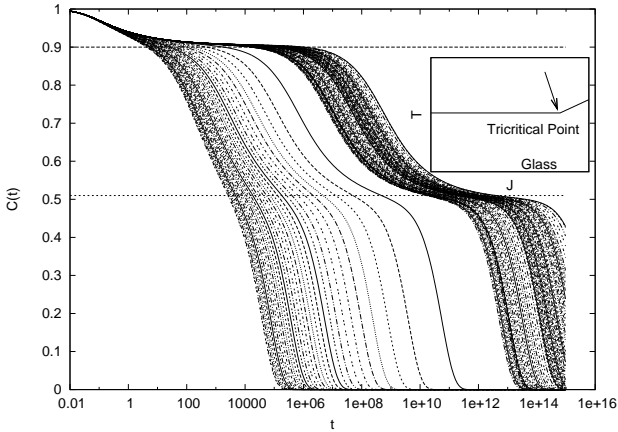


Fig. 4. Correlation function vs. time on log-scale in a cooling procedure in the $T/J_s, J_p/J_s$ phase diagram with $s = 3$ and $p = 16$ along a path perpendicular to the right hand side fluid/glass dynamic transition line, ending at the tricritical point $(0.61234, 1.1446)$.

titative differences can be non-negligible). A first plateau, q_1 , occurs for $t \gtrsim t_\gamma$ and a second one, $q_2 < q_1$, on the characteristic time-scale at which the secondary relaxation occurs ($t \gtrsim t_\beta$). We, thus, study the behavior in T of the characteristic relaxation times for processes on different time-scales and their functional interrelation.

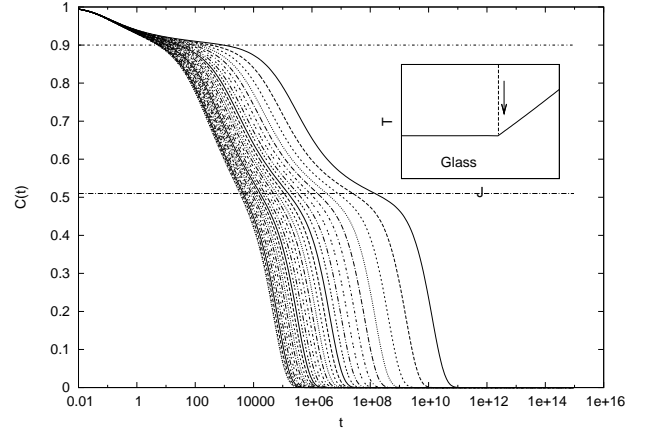


Fig. 5. Correlation function vs. time on log-scale in a cooling procedure in the $T/J_s, J_p/J_s$ phase diagram with $s = 3$ and $p = 16$ along the constant $J_{16} = 0.1446$ line, i.e. path perpendicular to the left hand side fluid/glass dynamic transition line ending at the tricritical point.

Near each plateau q_k the dynamical equation (10) predicts a power law behaviour of $C(t)$, with

$$C(t) - q_k \sim t^{-a_\kappa}, \quad (13)$$

for $C(t) \gtrsim q_k$, and the von Schweidler law:

$$C(t) - q_k \sim -t^{b_\kappa} \quad (14)$$

for $C(t) \lesssim q_k$. We can now expand the dynamical equation (10) about the plateaus in powers of $\phi(t) = C(t) - q_k$, with $\phi \ll 1$. To this aim, a suitable rescaled time $\tau = t/t_\kappa$, is introduced, where t_κ diverges at the critical point, and a relative rescaling function $g_\kappa(\tau)$, such that $\phi(t) \sim g_\kappa(\tau)\sqrt{\bar{r}(q) - \bar{r}}$, cf. App. A. Eventually one obtains the scaling equation

$$(1 - \bar{m}_\kappa)g_\kappa^2(\tau) + \int_0^\tau d\tau' [g_\kappa(\tau - \tau') - g_\kappa(\tau)] \frac{\partial g_\kappa(\tau)}{\partial \tau} = -1. \quad (15)$$

The parameter \bar{m}_k , also called "exponent parameter" λ in MCT, takes the exact expression

$$\bar{m}_\kappa = \frac{(1 - q_\kappa)^3}{2} A''(q_\kappa) \quad (16)$$

where the plateau correlations q_k are obtained from the self-consistency equations for the asymptotic dynamic solution for the 2RSB glass [28]. Inserting the expressions (13)-(14) of $g_k(t)$ into Eq. (15) one obtains the following relationships:

$$\bar{m}_\kappa = \frac{\Gamma^2(1 - a_\kappa)}{\Gamma(1 - 2a_\kappa)}; \quad 0 < a_\kappa < 1/2 \quad (17)$$

and

$$\bar{m}_\kappa = \frac{\Gamma^2(1 + b_\kappa)}{\Gamma(1 + 2b_\kappa)}; \quad 0 < b_\kappa < 1 \quad (18)$$

The analysis of the exponents for the two plateaus as the tricritical point is approached along the path perpendicular to the high J_{16} dynamic transition line is written in table 1 where we report their values for both plateaus. The approach to the tricritical point is not unique and the estimate of the exponents is usually very sensitive in MCT. This can be a possible cause for the mismatch between numerically interpolated and theoretically computed, cf., Eq. (16)

Moving to the frequency domain, the susceptibility loss, linked to the spectral densities by the Fluctuation - Dissipation Theorem $\chi''(\omega) = \omega/(2T)S(\omega)$ nearby the tricritical point displays two peaks as in the dielectric loss data of materials in which JG processes have been detected, cf., e.g., [15,13,14,35].

In Fig. 6 the development of the secondary peak is plotted as the tricritical point is approached in the T, J_p diagram. For small contribution from the p interaction only

Table 1. Mode coupling theory exponents of power-law relaxation to and from high and low plateau in correlation.

a_1	b_1	\bar{m}_1	a_1 (th)	b_1 (th)	\bar{m}_1 (th)
0.38(1)	0.89(1)	0.54(1)	0.38797	0.95045	0.5252
a_2	b_2	\bar{m}_2	a_2 (th)	b_2 (th)	\bar{m}_2 (th)
0.302(3)	0.55(1)	0.754 (6)	0.30441	0.55738	0.7505

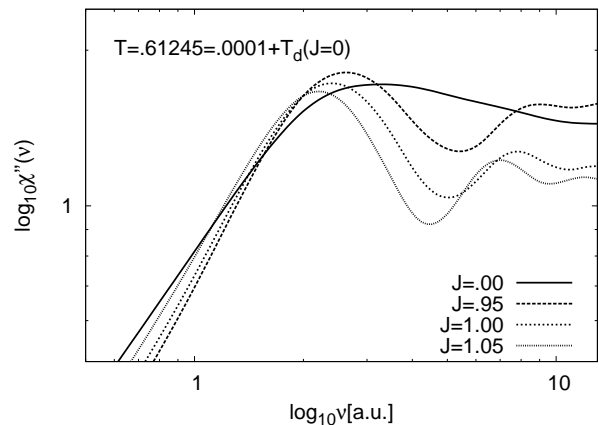


Fig. 6. Susceptibility loss in frequency ω at constant temperature $T = 0.0001 + T_d(J_{16} = 0)$ and different values of J_{16}/J_3 .

the α peak is pronounced near the transition of dynamic arrest. As the p -body interaction increases in strength and the tricritical point is approached a secondary β peak arises.

3 Interrelation between relaxation times

From the times at which the correlation decays from each well separated plateau we can investigate the possibility of a functional relationship among them. In Ngai's Coupling Model [35,36], the evidence of a deep link between

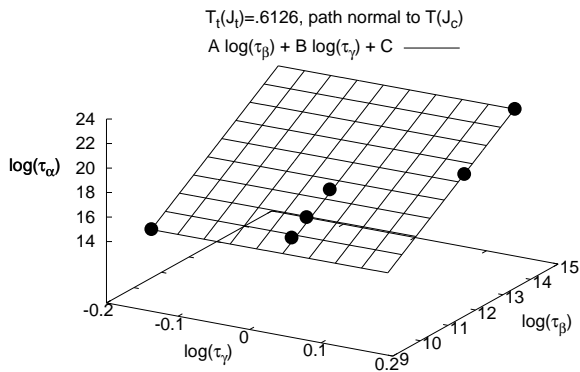


Fig. 7. Interrelation between the characteristic relaxation times of the fast (γ), Johari-Goldstein (β) and fully cooperative (α) processes.

secondary and structural processes is, e.g., connected to a strong stretch in the exponential relaxation to equilibrium in supercooled liquids [37][38]

$$C_{KWW}(t) = \exp \left\{ - \left(\frac{t}{\tau} \right)^{1-n} \right\} \quad (19)$$

by the law

$$\tau_\alpha = [t_c^{-n} \tau_\beta]^{1/(1-n)}; \quad 0 < n < 1, \quad (20)$$

with t_c the time at which fast Maxwell-Debye exponential relaxation matches KWW relaxation. The larger is n , the more the peak at high frequency (short times) is pronounced. As n is small no peak related to secondary processes is appreciated.

In our model the structural relaxation to equilibrium turns out to be purely exponential also very near the dynamic transition temperature. However, the relaxation at time scales larger than the τ_β (decay from highest plateau) does present a non-exponential behavior containing, on top of the final fully cooperative relaxation at τ_α , also the relaxation to the lowest plateau (where β processes

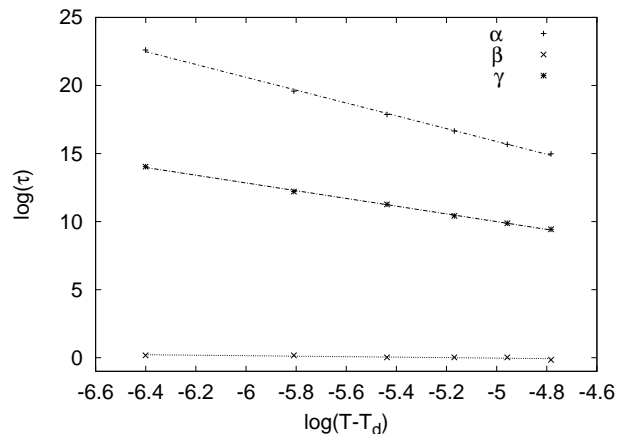


Fig. 8. Behavior of τ_α , τ_β and τ_γ vs $T - T_d^{(3c)}$ along the phase diagram path perpendicular to the fluid/1RSB_{II} dynamic transition line approaching the tricritical point.

are thermalized and α are completely stuck) and the decay from it, that follows the von Schweidler law, cf. Eq. (14).¹ In this respect, the stretched exponential might still be recovered and considered as an uneducated guess for the actual multi-time-scales dynamics. An alternative estimate of n would then support such conjecture. As a matter of fact, the relationship between fast, secondary and structural processes appears to qualitatively follow Ngai's law, Eq. (20) in a generic form:

$$\log \tau_\alpha = \beta_0 \log \tau_\beta + \gamma_0 \log \tau_\gamma \quad (21)$$

In Fig. 7 we plot the inter-dependence of the relaxation times of separated processes and the dependence on $\log \tau_\alpha$ on $\log \tau_\beta$ and $\log \tau_\gamma$ turns out to lie on a plane (with $\log \tau_\gamma$ almost constant), confirming Eq. (21).

¹ In MCT, it is, actually, common that stretched exponential relaxation only occurs at high wave-numbers. In our model we do not implement the wave-number dependence (we operate in the long distance limit).

In our description the time-scales over which one kind of process is active are well defined by characteristic times of relaxation to the plateaus. Cage rattling dynamics is thermalized already at the higher plateau of the correlation function and its equilibration time τ_γ does not depend on the distance from the dynamic critical point, cf. Fig. 8.

Slower JG processes (of intermolecular origin) [1][39] take place when structural relaxation is completely stuck and are strongly correlated off-equilibrium for a time such that $C(t) \simeq q_2$. Their characteristic time grows several order of magnitude, yet remaining several order of magnitudes smaller than τ_α , cf., Fig. 8. After that they relax to equilibrium on the characteristic time τ_β and the total correlation decreases to a second plateau q_1 where the longest processes, the cooperative α processes, remain off-equilibrium until $C(t) \simeq q_1$. Eventually, structural relaxation goes towards equilibrium, on the characteristic time-scale τ_α .

4 Conclusions

We presented a model with an undercooled fluid phase that can display both processes evolving on two and on three well separated time-scales depending on the region of phase diagram analyzed and allows for continuous interpolation between these two extreme situations. The model describes qualitatively quite well the phenomenology of viscous liquids in presence of secondary β processes. In particular, susceptibility loss shows a distinct secondary peak when the system is near the region of double time-scale bifurcation (i.e., near the tricritical point

across which the 2RSB glass can be reached). This signal is smeared going far from the tricritical point, changing into an excess wing shape, as it has been by schematic MCTs so far, cf. e.g., [40,11], based on the Sjögren model [41,42].

The solution of thermodynamics of the model below the dynamic transition consists of a hierarchical nesting of processes evolving on completely different time-scales [22,28]. Such property hints that, even though taking place on separated time-scales, fast processes have a relevant influence on slow processes also near T_d from above. This observation naturally leads to a comparison with Ngai's Coupling Model [35,36] and stimulates a reflection on the way slow processes dynamics combine into a stretched exponential, or, similarly, a Cole-Davidson representation of the relaxation in glassy systems.

In our disordered s - p -spherical spin model we find that α and β relaxation processes do stay apart, cf. Fig. 8, down to the dynamic transition, whose counterpart in realistic glass formers is the crossover temperature where the separation of time-scales begins to *accelerate* [34,43]. The relaxation time τ_β , actually, increases of several order of magnitude but τ_α also increases and accelerates faster than τ_β . This is apparently in contrast with the observation of Stevenson and Wolynes [12] that approaching T_d (the finite-dimensional analogue of T_d , to be precise) β process becomes the dominant mode in structural relaxation and the cooperativeness of α and β is not distinguishable anymore. Since that result is obtained in the framework of random first order transition systems, to

which our model belongs, further investigation is needed to understand the origin of possible substantial differences.

Acknowledgements

The authors thank Simone Capaccioli, Kia Ngai and Emanuela Zaccarelli for stimulating discussions. The research leading to these results has received funding from the Italian Ministry of Education, University and Research under the Basic Research Investigation Fund (FIRB/2008) program/CINECA grant code RBFR08M3P4.

A Dynamic scaling equation near plateaus

Let us define the function $\bar{r}(q)$

$$\bar{r}(q) = \frac{1}{1-q} - \Lambda(q) \quad (22)$$

where Λ is defined in Eq. (12), related to the longest solution $q = \lim_{t \rightarrow \infty} C(t)$ of (10) through

$$\bar{r}(q) = \bar{r}. \quad (23)$$

The solution to the above equation corresponds to a minimum of $\bar{r}(q)$ ($\bar{r}'(q) = 0$). Derivatives of $\bar{r}(q)$ take the form

$$\frac{d^m \bar{r}(q)}{dq^m} = \frac{m!}{(1-q)^{m+1}} - \frac{d^m \Lambda(q)}{dq^m}. \quad (24)$$

Writing $C(t) = q + \phi(t)$ we can expand $\Lambda[C(t)]$ near q , for small ϕ :

$$\Lambda(q + \phi) = \sum_{m=0}^{\infty} \frac{\Lambda^{(m)}(q)}{m!} \phi^m \quad (25)$$

where

$$\Lambda^{(m)} \equiv \frac{d^m \Lambda(q)}{dq^m} \quad (26)$$

In Eq. (10) we can, thus, rewrite the integral

$$\int_0^t dt' \Lambda[C(t-t')] \partial_{t'} \phi(t') = -(1-q)\Lambda(q) \quad (27)$$

$$+ \sum_{m=1}^{\infty} \left[\frac{\Lambda^{(m-1)}(q)}{(m-1)!} - (1-q) \frac{\Lambda^{(m)}(q)}{m!} \right] \phi^m(t) \\ + \sum_{m=1}^{\infty} \frac{\Lambda^{(m)}(q)}{m!} I_m(t)$$

$$I_m(t) \equiv \int_0^t dt' [\phi^m(t-t') - \phi^m(t)] \partial_{t'} \phi(t') \quad (28)$$

where $I_m(t) = O(\phi^{m-1}(t))$.

Expanding equation (10) in powers of $\phi(t)$ and using Eq. (27), after a few algebraic steps we obtain

$$\Gamma_0^{-1} \partial_t \phi(t) + [\bar{r} + \Lambda(q) - (1-q)\Lambda^{(1)}(q)] \phi(t) \\ + \sum_{m=2}^{\infty} \left[\frac{\Lambda^{(m-1)}(q)}{(m-1)!} - (1-q) \frac{\Lambda^{(m)}(q)}{m!} \right] \phi^m(t) \\ + \sum_{m=1}^{\infty} \frac{\Lambda^{(m)}(q)}{m!} I_m(t) = (1-q) [\bar{r} + \Lambda(q)] - 1. \quad (29)$$

From (24), defining γ_m and δ_m as follows

$$\gamma_m \equiv \frac{1}{(1-q)^{m-2}} \quad (30)$$

$$\delta_m \equiv \frac{(1-q)^3}{m!} \frac{d^m}{dq^m} [\bar{r}(q) - r],$$

we can rewrite

$$\frac{\Lambda^{(m)}(q)}{m!} = \frac{1}{(1-q)^3} (\gamma_m - \delta_m). \quad (31)$$

Inserting Eq. (31) in Eq. (29) we find

$$\Gamma_0^{-1} \partial_t \phi(t) + \frac{1}{(1-q)^3} \sum_{m=1}^{\infty} [-\delta_{m+1} (1-q)\delta_m] \phi^m(t) \\ + \frac{1}{(1-q)^3} \sum_{m=1}^{\infty} [\gamma_m - \delta_m] I_m(t) = -\frac{\delta_0}{(1-q)^2} \quad (32)$$

that, at the order ϕ^2 , becomes

$$\Gamma_0^{-1} \partial_t \phi(t) + \frac{1}{(1-q)^3} [-\delta_0 + (1-q)\delta_1] \phi(t) \quad (33)$$

$$+ \frac{1}{(1-q)^3} [-\delta_1 + (1-q)\delta_2] \phi^2(t)$$

$$+ \frac{1}{(1-q)^3} (\gamma_1 - \delta_1) I_1(t) + o(\phi^3) = -\frac{\delta_0}{(1-q)^2}.$$

If $\bar{r}(q)$ develops a local minimum we have

$$\bar{r}'(q) = \delta_1 = 0 \quad (34)$$

near the minimum $\bar{r}(q) - \bar{r} \ll 1$ and consequently we define the small quantity

$$\sigma \equiv \delta_0 = (1 - q)^3 [\bar{r}(q) - \bar{r}] \ll 1. \quad (35)$$

Defining the quantity

$$\bar{m} \equiv \frac{(1 - q)^3}{2} A''(q) \quad (36)$$

we can, further, write

$$\delta_2 = 1 - \bar{m}. \quad (37)$$

We can rewrite Eq. (33) as follows

$$\begin{aligned} \Gamma_0^{-1} \partial_t \phi(t) - \frac{\sigma}{(1 - q)^3} \phi(t) \\ + \frac{1}{(1 - q)^2} [(1 - \bar{m}) \phi^2(t) + I_1(t)] + o(\phi^3) = -\frac{\sigma}{(1 - q)^2} \end{aligned} \quad (38)$$

when $\sigma \rightarrow 0$ the solution of Eq. (38) is of the form

$$\phi(t) = \sigma^{1/2} g(\tau), \quad \tau = t/t_\sigma = o(1) \quad (39)$$

where $g(\tau)$ is solution of the following scaling equation:

$$(1 - \bar{m}) g^2(t) + \int_0^\tau d\tau' [g(\tau - \tau') - g(\tau)] \partial_{\tau'} g(\tau') = -1. \quad (40)$$

If the dynamic equation develops a solution with two plateaus at the values g_κ (with $\kappa = 1, 2$), we can fix two rescaled time scales τ_κ where $t/t_{\sigma_\kappa} = o(1)$ and we can generalize Eq. (40) to Eq. (15)

$$(1 - \bar{m}_\kappa) g_\kappa^2(t) + \int_0^\tau d\tau' [g_\kappa(\tau_\kappa - \tau') - g_\kappa(\tau_\kappa)] \partial_{\tau'} g_\kappa(\tau') = -1. \quad (41)$$

References

1. G. Johari, M. Goldstein, J. Chem. Phys. **53**, 2372 (1970)
2. G. Johari, M. Goldstein, J. Phys. Chem. **74**, 2034 (1970)
3. G. Johari, M. Goldstein, J. Chem. Phys. **55**, 4245 (1971)
4. J. Wong, C. Angell, *Glass: structure by spectroscopy* (Dekker (New York), 1974)
5. S. Adichtchev, T. Blochowicz, C. Gainaru, V.N. Novikov, E.A. Ressler, C. Tschirwitz, Journal of Physics: Condensed Matter **15**, S835 (2003)
6. T. Blochowicz, C. Tschirwitz, S. Benkhof, E. Ressler, J. Chem. Phys. **118**, 7544 (2003)
7. S. Adichtchev, T. Blochowicz, C. Tschirwitz, V.N. Novikov, E.A. Rössler, Phys. Rev. E **68**, 011504 (2003)
8. K. Ngai, P. Lunkenheimer, C. Leon, U. Schneider, R. Brand, L. A. J. Chem. Phys. **115**, 1405 (2001)
9. K. Ngai, M. Paluch, J. Chem. Phys. **120**, 857 (2004)
10. H. Cummins, J. Phys.: Condens. Matter **17**, 1457 (2005)
11. W. Götze, M. Sperl, Phys. Rev. Lett. **92**, 105701 (2004)
12. J. Stevenson, P. Wolynes, Nature Physics **6**, 62 (2010)
13. J. Wiedersich, T. Blochowicz, S. Benkhof, A. Kudlik, N. Surotsev, C. Tschirwitz, V. Novikov, E. Rössler, J. Phys.: Condens. Matter **11**, A147 (1999)
14. A. Kudlik, C. Tschirwitz, T. Blochowicz, S. Benkhof, E. Rössler, J. Non-Cryst. Solids **235-237**, 406 (1999)
15. R. Nozaki, D. Suzuki, S. Ozawa, Y. Shiozaki, J. Non-Cryst. Solids **235-237**, 393 (1998)
16. T.R. Kirkpatrick, D. Thirumalai, Phys. Rev. B **36**, 5388 (1987)
17. T.R. Kirkpatrick, D. Thirumalai, P.G. Wolynes, Phys. Rev. A **40**, 1045 (1989)
18. A. Crisanti, H. Sommers, Z. Phys. B **87**, 341 (1992)

19. A. Crisanti, H. Horner, H. Sommers, *Z. Phys. B* **92**, 257 (1993)
20. J.P. Bouchaud, L. Cugliandolo, J. Kurchan, M. Mézard, *Physica A* **226**, 243 (1996)
21. V. Krakoviack, *Phys. Rev. B* **76**, 136401 (2007)
22. A. Crisanti, L. Leuzzi, *Phys. Rev. B* **76**, 184417 (2007)
23. A. Crisanti, L. Leuzzi, *Phys. Rev. B* **76**, 136402 (2007)
24. M.J. Greenall, M.E. Cates, *Phys. Rev. E* **75**, 051503 (2007)
25. A. Crisanti, L. Leuzzi, *Phys. Rev. Lett.* **93**, 217203 (2004)
26. A. Crisanti, L. Leuzzi, *Phys. Rev. B* **73**, 014412 (2006)
27. W. Götze, *Complex Dynamics of glass forming liquids. A mode-coupling theory* (Oxford University Press (Oxford, UK), 2009)
28. L. Leuzzi, *Philos. Mag.* **88**, 4015 (2008)
29. H. Sompolinsky, *Phys. Rev. Lett.* **47**, 935 (1981)
30. H. Sompolinsky, A. Zippelius, *Phys. Rev. B* **25**, 6860 (1982)
31. P. Martin, E. Siggia, H. Rose, *Phys. Rev. A* **8**, 423 (1973)
32. C. De Dominicis, *Physics Reports* **67**, 37 (1980)
33. A. Crisanti, *Nuclear Physics B* **796**, 425 (2008)
34. E. Donth, *The Glass Transition* (Springer (Berlin), 2001)
35. K. Ngai, *J. Phys.: Condens. Matter* **15**, S1107 (2003)
36. K. Ngai, S. Capaccioli, *Phys. Rev. E* **69**, 031501 (2004)
37. R. Kohlrausch, *Pogg. Ann. Phys.* **12**, 393 (1847)
38. G. Williams, D. Watts, *Trans. Faraday Soc.* **66**, 80 (1970)
39. G. Johari, *J. Chem. Phys.* **58**, 1766 (1973)
40. W. Götze, M. Sperl, *Phys. Rev. E* **66**, 011405 (2002)
41. L. Sjögren, *Phys. Rev. A* **33**, 1254 (1986)
42. W.G. Götze, L. Sjögren, *J. Phys. Condens. Matter* **1**, 4183 (1989)
43. L. Leuzzi, T. Nieuwenhuizen, *Thermodynamics of the glassy state* (Taylor & Francis, 2007)